Biochimica et Biophysica Acta 1862 (2016) 1994–2003

Contents lists available at ScienceDirect

Biochimica et Biophysica Acta

journal homepage: www.elsevier.com/locate/bbadis

pH-sensitive K^+ channel TREK-1 is a novel target in pancreatic cancer

Daniel R.P. Sauter [a,b,1,2], Christiane E. Sørensen [a,1], Markus Rapedius [b], Andrea Brüggemann [b], Ivana Novak [a,*]

[a] Section for Cell Biology and Physiology, Department of Biology, Universitetsparken 13, University of Copenhagen, DK-2100 Copenhagen Ø, Denmark
[b] Nanion Technologies GmbH, Gabrielstr. 9, 80636 Munich, Germany

ARTICLE INFO

Article history:
Received 1 October 2015
Received in revised form 16 June 2016
Accepted 15 July 2016
Available online 19 July 2016

Keywords:
K_{2P} channel
K^+ channel
BL1249
Pancreatic adenocarcinoma
Proliferation
Migration

ABSTRACT

Pancreatic ductal adenocarcinoma (PDAC) is one of the most lethal cancers and new therapeutic targets are urgently needed. One of the hallmarks of cancer is changed pH-homeostasis and potentially pH-sensors may play an important role in cancer cell behavior. Two-pore potassium channels (K_{2P}) are pH-regulated channels that conduct a background K^+ current, which is involved in setting the plasma membrane potential (V_m). Some members of the K_{2P} superfamily were reported as crucial players in driving tumor progression. The aim of this study was to investigate pH-regulated K^+ currents in PDAC cells and determine possible effects on their pathological phenotype. Using a planar high-throughput patch-clamp system (SyncroPatch 384PE) we identified a pH-regulated K^+ current in the PDAC cell line BxPC-3. The current was inhibited by extracellular acidification and intracellular alkalization. Exposure to a set of different K^+ channel inhibitors, and the TREK-1 (K_{2P}2.1)–specific activator BL1249, TREK-1 was identified as the main component of pH-regulated current. A voltage-sensor dye (VF2.1.Cl) was used to monitor effects of pH and BL1249 on V_m in more physiological conditions and TREK-1–mediated current was found as critical player in setting V_m. We assessed a possible role of TREK-1 in PDAC progression using cell proliferation and migration assays and observed similar trends with attenuated proliferation/migration rates in acidic (pH < 7.0) and alkaline (pH > 7.4) conditions. Notably, BL1249 inhibited both PDAC cell proliferation and migration indicating that hyperpolarization of V_m attenuates cancer cell behavior. TREK-1 may therefore be a promising novel target for PDAC therapy.

© 2016 The Authors. Published by Elsevier B.V. This is an open access article under the CC BY-NC-ND license (http://creativecommons.org/licenses/by-nc-nd/4.0/).

1. Introduction

Pancreatic ductal adenocarcinoma (PDAC), the most common pancreas cancer form, is one of the most fatal cancer forms with >95% mortality and <5% survival rate in 5 years [6]. Despite intensive research efforts, the success rate of treatment remains low. One of the reasons for this severity is the high metastatic potential of this cancer. Ion channels are crucial players in supporting cell migration and proliferation and thus also metastasis formation [30,35,46]. In recent years, numerous reports have linked expression and function of several ion channels to disease state and progression [5,10,53,60].

One of the increasingly recognized hallmarks of cancer is its dysregulated pH homeostasis. Due to higher proliferative and glycolytic rates, cancer cells generate increasing amounts of metabolic acid. This is accompanied by a change in plasma membrane ion pumps and transporter expression and/or activity that promote H^+ efflux, thereby resulting in high (>7.4) intracellular pH (pH_i) and low (~6.7–7.1) extracellular pH (pH_e) [20,38,57,61]. This changed concentration gradient is known to be permissive for tumor progression and since this feature is unique to tumors, pH-sensing proteins may serve as valuable new targets in cancer therapy [61]. Albeit many proteins contain side chains with protonation state depending on pH value, only a few can be considered "true" pH sensors that influence cell behavior.

K^+ channels play pivotal roles in cell behavior linked to tumor progression [35,46,55], including regulation of cell cycle progression [25], migration [29], apoptosis [28] as well as angiogenesis [39]. Two-pore domain K^+ channels (K_{2P}) are of particular interest, as they conduct outward background K^+ currents and are activated throughout the entire range of membrane potentials [36]. Importantly, K_{2P} channels are sensitive to pH and have hence a direct effect on membrane potential, ion transport, volume regulation and Ca^{2+} homeostasis that are important for the physiological response of cells. In addition, K_{2P} channels have impact on cell survival and cell migration that is relevant in cancer progression. For example, Alvarez-Baron and colleagues observed an upregulation of TASK-2 (K_{2P}5.1) in response to 17 β–estradiol in MCF-7 and T47D breast cancer cell lines that was linked to cell proliferation [1]. Voloshyna et al. also reported a pro-proliferative role of a K_{2P} channel; prostatic carcinoma tissue showed TREK-1 (K_{2P}2.1) expression that was devoid in adjacent healthy prostatic gland tissue. Moreover, these workers also found that proliferation was decreased in PC3 (prostatic cancer cell line) when overexpressed with a dominant-negative

* Corresponding author at: Section for Cell Biology and Physiology, Department of Biology, University of Copenhagen, August Krogh Building, Universitetsparken 13, 2100 Copenhagen Ø, Denmark.
E-mail address: INovak@bio.ku.dk (I. Novak).
[1] These authors contributed equally.
[2] Present address: Sophion, Biolin Scientific, Baltorpsvej 154, DK-2750 Ballerup, Denmark.

http://dx.doi.org/10.1016/j.bbadis.2016.07.009
0925-4439/© 2016 The Authors. Published by Elsevier B.V. This is an open access article under the CC BY-NC-ND license (http://creativecommons.org/licenses/by-nc-nd/4.0/).

version of the channel [60]. Most work linking K_{2P} channel to cancer cell behavior has been done on TASK-3 (K_{2P}9.1). High expression levels were reported in breast, colon, lung and melanoma cells and channels affected proliferation, apoptosis, migration and mitochondrial function [27,29,42,43].

In the pancreas, alkaline-activated TALK-1 and 2, and TASK-2 are expressed as shown from RNA analysis and in situ hybridization [15]. Moreover, groups of Duprat and Lesage assessed TASK-1 and TREK-2 expression, respectively, in different human tissues using Northern Blot analysis. For both channels, most prominent expression was found in the pancreas [16,33]. It was postulated that in the healthy pancreas, TASK-2 (K_{2P}5.1) could play a crucial role in setting the electrical driving force for electrogenic HCO_3^- secretion and serve as an efflux pathway for K^+ [21]. Williams et al. investigated K_{2P} channel expression in the pathological state of the pancreas; using a data-mining approach they showed that in pancreatic cancer, TWIK-1 is over-expressed and TASK-1 is under-expressed. To our best knowledge, so far there are no functional studies investigating a possible role of K_{2P} channels in pancreatic cancer progression (or in fact pancreas physiology). Therefore, the aim of the present investigation was to characterize the effects of altered pH on K^+ currents and membrane potentials, and pharmacologically characterize the underlying channel. A further aim was to determine effects of K_{2P} channels on behavior of PDAC cells with the perspective to identify novel targets for pharmacological treatment.

2. Materials and methods

2.1. Cell culture

All cell lines were grown at 37 °C and 5% CO_2/air. Immortalized human pancreatic ductal epithelium (HPDE) (originally denoted H6c7 cell line) [18,45] cell line was cultured in keratinocyte serum-free medium supplemented by epidermal growth factor and bovine pituitary extract (Life Technologies, Inc., USA). BxPC-3 and AsPC-1 (ATCC, Germany) cells were grown in Roswell Park Memorial Institute medium with stable glutamine (RPMI 1640/Biochrom, Germany) and Capan-1 cells in Iscove's Modified Dulbecco's Medium (IMDM-1640/Biochrom, Germany), all were supplemented with 10% *v/v* (20% for Capan-1) Fetal Bovine Serum "Gold" (PAA Laboratories GmbH, Germany) and 1% *v/v* penicillin and streptomycin. Cells were passaged every 4–6 days by gentle trypsinization.

2.2. Electrophysiology

All whole-cell recordings were performed on the SyncroPatch 384PE (Nanion Technologies/Germany). Data acquisition and analysis was performed with the proprietary software PatchControl 384 and DataControl 384, respectively (Nanion Technologies/Germany). All recordings were carried out using planar borosilicate glass patch clamp chips [14] in a 384 microtiter plate format with resistances that corresponded to those of a conventional patch-pipette with 4–6 MΩ. For recordings, standard intracellular-like solution contained (in mM): 50 KCl, 60 KF, 10 NaCl, 20 EGTA and 10 HEPES (pH 7.2) and standard extracellular solution contained in mM: 140 NaCl, 4 KCl, 2 $CaCl_2$, 1 $MgCl_2$, 5 Glucose and 10 HEPES (pH 7.4). To adjust pH-values of intra- and extracellular solutions, buffers with different pKa were added to the above solution and titrated to final pH values (calculated osmolalities were comparable). These buffers were used: 5 mM 2-(N-morpholino)ethanesulfonic acid (MES) was used for pH 6.5 and 6.7; 5 mM 4-(2-hydroxyethyl)-1-piperazineethanesulfonic acid (HEPES) for pH 7.2 and 7.4 and 5 mM tris(hydroxymethyl) aminomethane (TRIS) for pH 8.5 and 9.0. For studies of pH_e-dependence, 50% of the volume of each of the 384 wells was replaced by a solution of given proton concentration that would result in the desired pH value (e.g. solution of pH 9.0 and pH 7.4 result in pH 8.5). For studies on intracellular pH (pH_i), the internal perfusion system was used to completely exchange the intracellular solution with a solution of desired pH_i value. Prior to the electrophysiological measurements cells were harvested by a gentle trypsinization. The cell suspensions were kept in the dedicated cell reservoir at 18 °C and shaken at 200 rpm in 50/50 *v/v* culture media/standard external solution. Each cell preparation was used for no longer than 3 h. For experiments, 10 μl of cell suspension was added to each well resulting in a final concentration of 50,000–80,000 cells/ml. To foster seal formation, high Ca^{2+} (25 mM) solution was applied externally and immediately washed out thoroughly. Only cells with a seal resistance $R_{seal} > 500$ MΩ were considered for analysis. Current was elicited using voltage-ramps from $V_{out} = -120$ to $+60$ mV with 1 s duration and $V_{hold} = -80$ mV. Data were later corrected for the calculated liquid junction potential (V_{LJ}).

2.3. Cell proliferation assay

To assess cell proliferation, cells were plated in triplicates on a 96-well plate and incubated overnight in 100 μl of respective culture medium at 37 °C and 5% CO_2/air. Next, cells were exposed to media of different pH-values for 24 h. pH-value was adjusted using different buffers MES (25 mM = pH 6.5; 20 mM = pH 6.7), HEPES (25 mM = pH 7.0; 20 mM = pH 7.2) or TRIS (20 mM = pH 8.2; 25 mM = pH 8.5). pH was stable during the duration of the experiment. Additionally, cells were exposed to different concentrations of BL1249 as indicated, or to siRNA for TREK-1 (see Section 2.6 for details). BrdU incorporation was measured using Cell Proliferation ELISA, BrdU (chemiluminescent) (Roche Diagnostics A/S, Denmark) following the manufacturer's instructions.

2.4. Scratch wound healing assay

BxPC-3 cells were plated in Essen Imagelock 96-well plates at 75,000 cells/well and incubated for 24 h at 37° C and 5% CO_2/air. Confluent monolayers were scratched using the Woundmaker (Essen Bioscience, USA), immediately washed two times with phosphate buffered saline (PBS) and incubated with the respective culture medium. pH-values were adjusted as described in "Cell Proliferation". Wound closure was followed for 48 h by time-lapse microscopy using the Incucyte (Essen Bioscience, USA) imaging system. Measurements were carried out in triplicates and data are represented as relative wound closure (%RWD) according to the following relationship $\%RWD = 100 \times w(t) - w(0) / c(t) - w(t)$. Here, w(t) represents the density of wounded area at time t and c(t) is the density of cell region at time t.

2.5. Measurements of the membrane potential (V_m)

Cells were seeded on glass coverslips at approximately 30–50% confluency and incubated at 37° C and 5% CO_2/air for at least 12 h. V_m was determined using voltage dye VF2.1.Cl [41], which was a kind gift from R. Tsien. VF2.1.Cl in DMSO was added to the media to 200 nM final concentration and cells were incubated for 20 to 50 min. BxPC-3 cells were subsequently washed with solution (containing in mM: 150 NaCl, 6 KCl, 1.5 $CaCl_2$, 1 $MgCl_2$, 10 HEPES and 10 Glucose) and mounted in a perfusion chamber. Changes in V_m were measured using TIRF iMIC microscope (TILL Photonics, Germany). VF2.1.Cl loaded cells were illuminated for 100 ms in 2 s intervals at $\lambda_{ex} = 470$ nm using TILL Polychrome monochromator. Fluorescence was collected between 515 and 565 nm on an image-intensifying, charge-coupled device (CCD) camera (TILL Photonics, Germany) and processed by an image processing system (TILL Photonics, Germany). LA Live Acquisition software was used to control monochromator and CCD camera. Changes in V_m are presented as $\Delta F/F_0$ (%), here F_0 represents the average value over the 30 first images (=1 min) and $\Delta F = F_0 - F$. Data was further corrected for fluorophore bleaching.

2.6. Western blot analysis

Protein samples, obtained from lysates of BxPC-3, Capan-1, HPDE, and HEK293 cells, were loaded on 10% Novex NuPAGE Bis-Tris precast polyacrylamide gels (Invitrogen). The HEK293 cells were stably transfected with human TREK-1 and served as positive control. For TREK-1 knockdown experiments 25 to 40 nM of the following three predesigned Mission siRNAs from Sigma-Aldrich were used individually or pooled: SASI_Hs02_00306750 (A), SASI_Hs01_00209726 (B), SASI_Hs02_00345240 (C), and Mission siRNA Universal Negative Control #1. For evaluation of transfection efficiency GAPDH siRNA (Mission siRNA SASI_Hs01_00140981) was used as positive control. Transfection was performed with DharmaFECT 1 Transfection Reagent (Dharmacon) according to the manufacturer's protocol. For Western blotting, protein was extracted from BxPC-3 cells 3 to 4 days after transfection. The protein samples were separated by electrophoresis, and subsequently blotted to Invitrolon PVDF membranes (Invitrogen). The membranes were blocked overnight at 4 °C in a 1:3 dilution of Blocking Buffer – Fish (BioFX, SurModics) in Tris-buffered saline (TBS) containing 0.1% Tween. Membranes were incubated with mouse monoclonal (1:200, Santa Cruz, sc-398449, TREK-1 (F-6)) primary antibody for 1 to 2 h at room temperature followed by washing and incubation with HRP-conjugated secondary antibody (1:2500 DAKO P0447, goat anti-mouse) for 1 to 2 h at room temperature. GAPDH #14C10 rabbit monoclonal antibody (Cell Signaling) was used as loading control. Chemiluminescence was detected by use of the EZ-ECL Detection Kit for HRP (Biological Industries), and imaged on Fusion FX (Vilber Lourmat). Band density was analyzed with Bio1D software.

2.7. Materials and statistical analysis

All inhibitors tested (except ruthenium red and tetrahexylammonium chloride) were dissolved in dimethyl sulfoxide (DMSO) as stock solutions and diluted appropriately to yield the final test concentrations and DMSO was <0.2% *v*/*v*. Ruthenium red and tetrahexylammonium chloride were dissolved in dH_2O. All compounds were obtained from Sigma-Aldrich (Germany). Results of multiple experiments are presented as means ± s.e.m., and statistical analysis was carried out by using one-way analysis of variance with Tukey's post-test, or Student's *t*-test, as appropriate. $P \leq 0.05$ was considered statistically significant.

3. Results

3.1. BxPC-3 cells exhibit pH_e-dependent K^+ current

We assessed the pH-dependence of currents in various PDAC cells (BxPC-3, Capan-1, AsPC-1) and an immortalized human pancreatic ductal epithelium cell line (HPDE) using a 384-well based planar patch clamp system (SyncroPatch 384PE/Nanion). BxPC-3 cells showed pH sensitivity as shown in Fig. 1. Other cells exhibited currents that were not sensitive to pH_e changes (Supplementary Fig. S1). Therefore, we pursued further high-throughput patch clamp studies on BxPC-3 cells. The tested BxPC-3 cells clustered into two distinct groups: approximately two-thirds of the measured cells were devoid of a notable K^+ current and reversed at the calculated reversal potential for Cl^- (E_{Cl}) (Fig. 1A). The remaining third (32 ± 2%, percentage calculated from results of 7 tested chips) exhibited a more hyperpolarized membrane potential (V_m) with reversal potential between E_{Cl} and E_K indicating a contribution of several current components (Fig. 1B). Change in extracellular pH (pH_e) from pH_e 7.4 to pH_e 8.5 resulted in an activation of an outward current only in the group of hyperpolarized cells (Fig. 1B). The following characterization concentrated only on the pH - sensitive cells. To verify that pH-sensitive current was mediated by K^+, we exposed alkali-activated cells to different concentrations of extracellular K^+ (K_{ext}) (Fig. 1C). As expected, the reversal potential (E_{rev}) changed

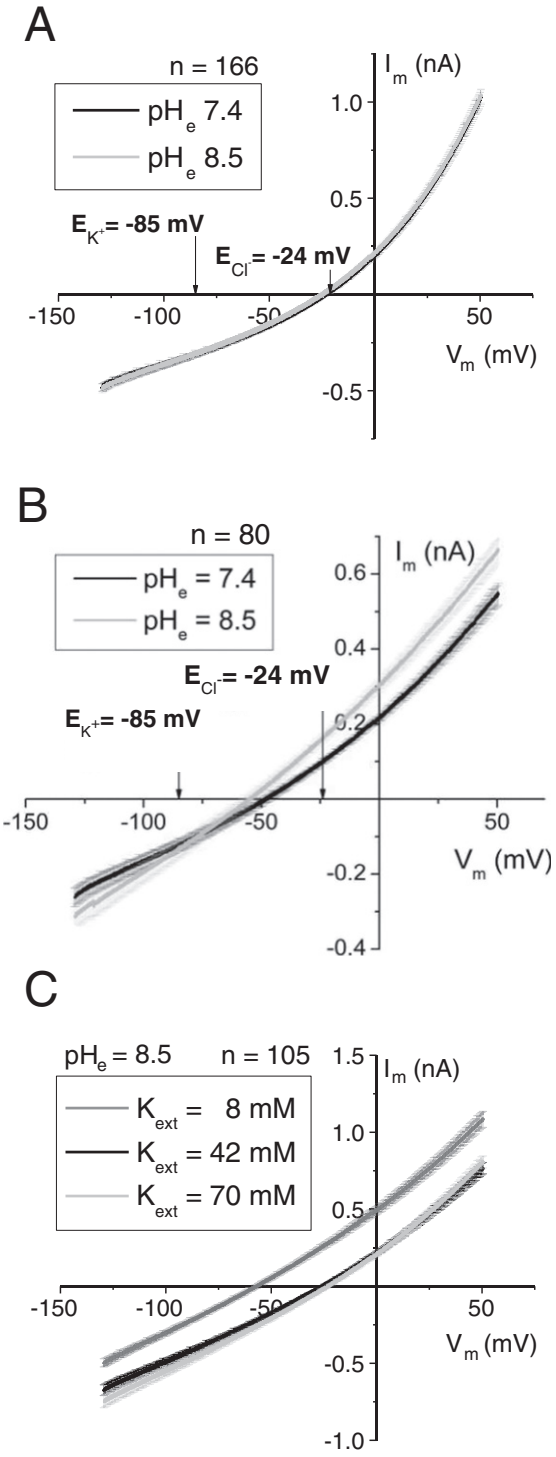

Fig. 1. BxPC-3 cells exhibit pH-sensitive K^+ current. Whole-cell patch clamp recordings of BxPC-3 cells in absence of $[Ca^{2+}]_i$. Calculated reversal potentials for Cl^- (E_{Cl}) and K^+ (E_K) are indicated with arrows. A: cells insensitive to change in pH_e. B: one third of cells were sensitive to pH_e. Traces were recorded after full saturation of pH_e-activated current. Percentage of cells showing pH-sensitive current was determined from each of the 7 measured 384-well chips (Student's *t*-test; $P = 5*10^{-7}$). C: pH_e-activated current present in different concentrations of external K^+ (K^+_{ext}). Data shown are mean of n experiments as indicated ± s.e.m.

to more positive values when K_{ext} was increased, however, E_{rev} did not get more positive than E_{Cl}, indicating basal activity of Cl^- channels.

To assess pH-dependence of current in BxPC-3 cells in more detail, cells were exposed to different pH_e-values and current change was followed using a voltage-ramp protocol (Fig. 2). The pH_e-sensitive

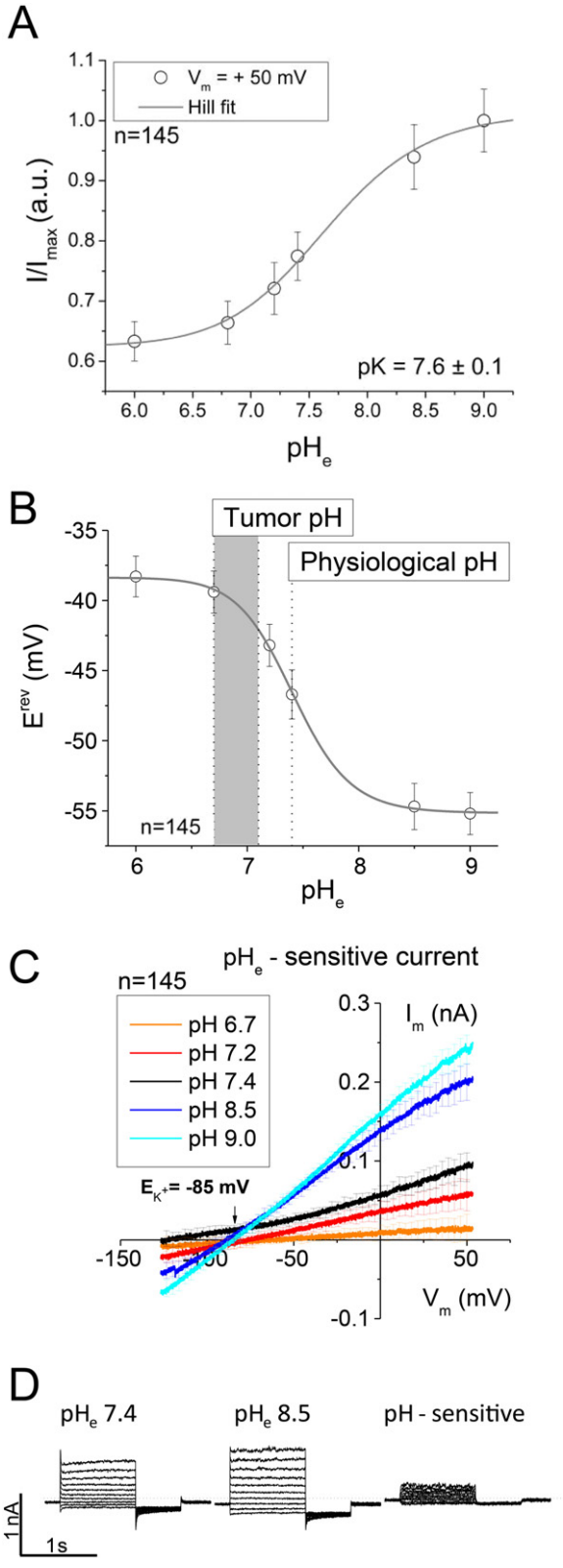

Fig. 2. BxPC-3 cells are sensitive to pH_e. Whole-cell patch clamp measurements of BxPC-3 cells. A: pH_e-dependence of K^+ current. I_{max} represents values measured at pH 9.0. B: pH_e-dependence of reversal potential (E_{rev}). Grey shaded area indicates pH values typical in tumor environments [61] and dashed line shows value in healthy tissue. C: pH_e-sensitive currents. Data was calculated by subtracting IV curve of pH 6.0 from those IV curves indicated. All sensitive currents reverse close to E_K. D: representative current traces over time. Current was elicited by a voltage-step protocol from −120 mV to +60 mV in increments of 20 mV. Data shown are mean of n experiments as indicated ± s.e.m.

current was fully activated at pH_e 9.0 and deactivated below pH_e 6.7. The pK value of the activation was calculated to 7.6 ± 0.1 (Fig. 2A). Fig. 2B highlights the importance of this pH_e-dependent current activation on the membrane potential; a step from a physiological pH_e 7.4 to values commonly observed in tumors, i.e. pH_e 6.7–7.1 [61], depolarized V_m by ≈5–8 mV. To rule out a possible pH-dependent Cl^- current, we analyzed pH_e–sensitive portion of this current (Fig. 2C). All pH_e–sensitive currents reversed close to E_K, suggesting that K^+ channels were sole mediators of this pH-sensitive current. Furthermore, pH-sensitive current showed very fast activation kinetics (Fig. 2D). These characteristics are best described by K^+ channels of the two-pore (K_{2P}) family [36].

Even though K_{2P} subtypes exhibit differences in pH_e-dependence, they are best distinguished by their pH_i dependence. Therefore, we exposed the cells to different pH_i values and recorded the current response in the whole-cell configuration. pH_i steps from 7.2 to 8.5 at physiological pH_e resulted in a complete inhibition of K^+ current ($E_{pHi8.5} \approx E_{Cl}$) (Fig. 3A). However, a very few cells (<5% of all cells tested) showed an opposite behavior (data not shown). Replacement of intracellular K^+ by Rb^+ was shown to shift the apparent pH_i–dependence of K_{2P} channel as Rb^+ stabilizes the selectivity filter gate [48]. Therefore, internally applied Rb^+ can be used to selectively activate K_{2P} channel. Substitution of 50 mM K^+ with Rb^+ evoked a large current in BxPC-3 cells (Fig. 3B), indicating the participation of K_{2P} channels. However, this current was not solely composed of K^+ as the Rb^+-sensitive portion reversed far from E_K. The quaternary ammonium compound, tetrahexylammonium chloride (ThexA) is a classical open channel blocker for voltage-gated K^+ (K_v) channels and a voltage-dependent blocker of the inward-rectifier K^+ (K_{ir}) channels [8,44]. Moreover, ThexA was recently identified as voltage-independent inhibitor of TRESK (K_{2P}18.1), TASK-3 and TREK-1 [48]. ThexA, when applied intracellularly, can hence be used to identify K_{2P} channels. In our experiments, 10 μM ThexA resulted in a pronounced inhibition of both outward and inward current (Fig. 3C).

To identify the subtype of a K_{2P} channel that mediates pH-sensitive current, we used a set of pharmacological tools and tested them on the pH 8.5 activated currents (Fig. 4A). The polycationic dye ruthenium red (2 μM) (inhibitor of TASK-3) and the antiarrhythmic drug carvedilol (5 μM) (inhibitor of TASK-1) had no effect on pH-activated current. On the other hand, application of quinine (50 μM) (inhibits TREK-1 and also other channels) and genistein (150 μM) (inhibits TASK-1 and 3) resulted in a moderate but significant reduction in outward current. Intracellular application of ThexA (10 μM) completely abolished the pH-activated current; i.e. outward currents reached same values as those measured at pH_e 6.0. Expression of TREK-1 proteins in different pancreatic ductal cell lines was confirmed using Western blot analysis (Fig. 4B). We further tested the TREK-1 –specific activator BL1249 (Fig. 4C–E). BL1249 application at pH_e 7.4 elicited an outward current that shifted E_{rev} towards E_K. We estimated the EC_{50} value of this activation to 2 ± 2 μM (n = 62). BL1249–sensitive current showed same current-over-time signature as observed for pH-sensitive current (Figs. 2D and 4E).

3.2. pH-regulated current controls V_m

In addition to patch-clamp studies with controlled intracellular compositions, we investigated the effect of pH on V_m of intact BxPC-3 cells in a more physiological set-up. Here we used bioimaging and a voltage-sensitive reporter dye VF2.1.Cl developed by R. Tsien [41]. Cells loaded with VF2.1.Cl (Fig. 5A) were exposed to physiological-like solution of different pH values and changes in V_m were followed using fluorescence microscopy (Fig. 5B). A change towards acidic pH-values increased fluorescence signal by 2.7 ± 0.2% (n = 172 cells of N = 3 independent experiments). Change of $\Delta F/F_0$ = 1% translates to ΔV_m = 40–50 mV [7,41], indicating depolarization of V_m as expected for this fluorophore [41]. Likewise, alkalization decreased fluorescence by 3.5 ± 0.1% and thus hyperpolarized V_m. These V_m changes are

consistent with closing and opening of K_{2P} channels such as TREK-1, respectively. In the same set-up we further tested BL1249 at pH_e 6.7 for its effect on V_m and results are shown in Fig. 5C. In line with observations of patch-clamp measurements, BL1249 hyperpolarized V_m with decrease in fluorescence of 6.7 ± 0.2% (n = 86 cells of N = 3 independent experiments). This BL1249-induced change in fluorescence corresponded approximately to the change in fluorescence detected by changes in pH_e from 6.7 to 8.2. Notably, albeit changes in V_m varied between BxPC-3 cells, all tested cells exhibited sensitivity to pH and BL1249. These V_m effects seen with the VF2.1.Cl fluorophore stand in contrast to results of patch-clamp measures where such sensitivity was only observed in ≈1/3 of the cells.

We also determined pH effects on V_m in HPDE and Capan-1 cells, detected with the voltage sensor (Supplementary Fig. S2). In both cell lines, extracellular acidification resulted in hyperpolarization of V_m rather than depolarization as observed in BxPC-3 cells. However, addition of BL1249 induced hyperpolarization in both cell types.

3.3. BL1249 inhibits BxPC-3 cell proliferation and migration

We investigated a possible role of pH-sensitive current in BxPC-3 cell behavior (Fig. 6). Using BrdU incorporation we estimated cell proliferation. Cells were cultured at different pH values for 24 h before BrdU incorporation was measured (Fig. 6A). Highest proliferation rate was observed at pH values between pH 7.0–7.4. Alkaline media slightly attenuated proliferation by 20 ± 6% and 27 ± 4% at pH 8.2 and pH 8.5, respectively. Acidic pH had a more pronounced impact with 72 ± 4% inhibition at pH 6.5 and 60 ± 20% at pH 6.7 (n = 3–4). Additional treatment with BL1249 (20 μM) further reduced BrdU incorporation, significantly at pH 7.0 and pH 7.4. We reasoned that the concentration of the compound could be sub-optimal, possibly due to binding to serum proteins. Therefore, we exposed cells to increasing concentrations of BL1249 at pH 7.4 (10% *v*/*v* serum). The activator inhibited cell BrdU incorporation in a dose-dependent manner with IC_{50} value of 60 ± 10 μM (n = 3–4) (Fig. 6B). These data indicate that BL1249 inhibited cell proliferation. Cells treated with siRNA against TREK-1 showed a tendency towards higher BrdU incorporation at pH 7.4 compared to cells treated with negative control RNA (Fig. 7A). Knockdown of the TREK-1 protein was evaluated by Western Blot (Fig. 7B). Densitometric analyses of the band at 45 kDa, obtained with the TREK-1 monoclonal antibody and normalized to GAPDH, are shown in Fig. 7C. For most siRNAs, we observed a moderate decrease in TREK-1 protein level when compared to the level in samples from cells treated with negative control RNA. Nevertheless, the reduction in TREK-1 protein expression by siRNA B and C was significant (Fig. 7C).

A possible role of pH-sensitive current in cell migration was assessed using scratch wound-healing assay with same conditions as described for proliferation and data are shown in Fig. 6C and D. To rule out that the observed effect was due to different growth rates at the different conditions, we inhibited proliferation by addition of 5 μM aphidicolin [58]. The results correlated with those obtained in the BrdU assay. The fastest wound closure was detected at pH-values between pH 7.0 and 7.4. Both at alkaline (pH 8.2 and pH 8.5) and acidic (pH 6.7) values, cells appeared to show attenuated migration, but no significance was reached (Fig. 6C). Addition of BL1249 (20 μM) did not appear to rescue this inhibitory trend nor did it amplify it significantly. Nevertheless, as shown in Fig. 6D, BL1249 decreased cell migration at pH 7.4 dose-dependently with an estimated IC_{50} concentration of 70 ± 50 μM.

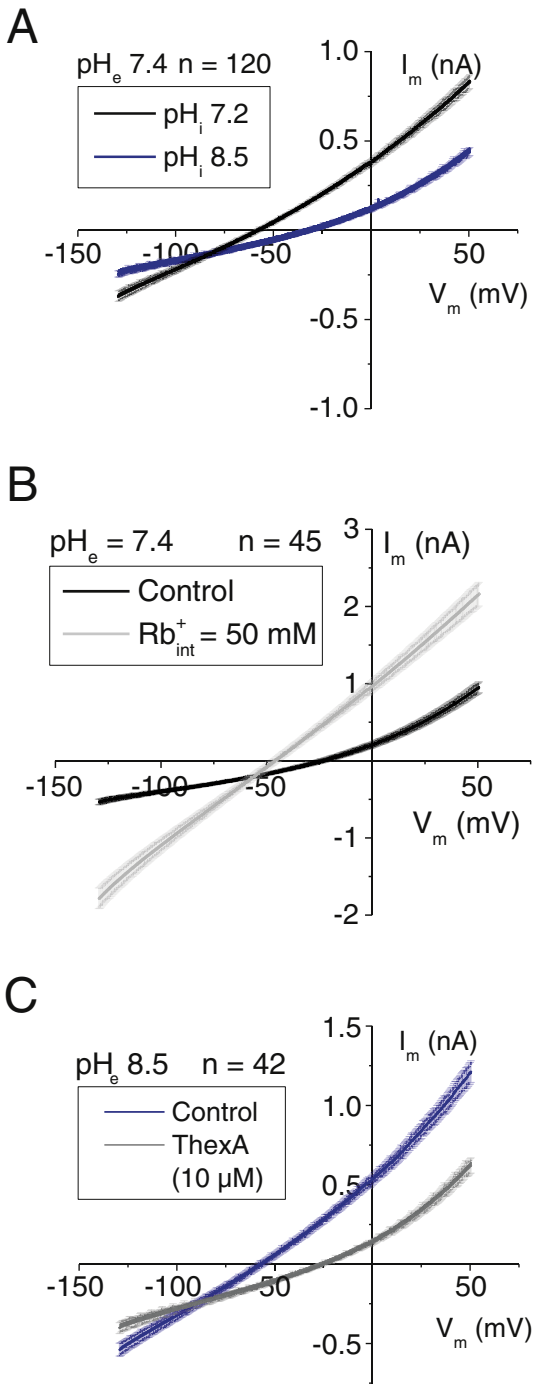

Fig. 3. Effect of intracellular alkalization, Rb^+ and ThexA on K^+ currents. Whole-cell patch clamp recording at different pH of intracellular test solutions. A: pH_i sensitivity at physiological pH_e. B: substitution of 50 mM intracellular K^+ with Rb^+ at physiological pH_e and pH_i. Rb^+ activates some of the K_{2P} channels (see text) C: intracellular application of tetrahexylammonium chloride (ThexA). Data shown are mean of n experiments as indicated ± s.e.m.

4. Discussion

In the present study, we identified a pH-sensitive K^+ current in the pancreatic cancer cell line BxPC-3 and provide strong evidence that this current is mediated by TREK-1. This study also presents the first functional report on the K_{2P} channel in pancreatic cells of exocrine origin. Below, we discuss a possible role of the channel in tumor proliferation and migration.

4.1. TREK-1 mediates pH-sensitive K^+ current in BxPC-3 cells

Change in pH_e elicited a current that shifted E_{rev} towards E_K. The pH-sensitive part of the current reversed almost exactly at E_K (Figs. 1B and 2C). A number of K^+ channels exhibit pH-sensitivity and could hence account for this observation. Some inward rectifier K^+ channels

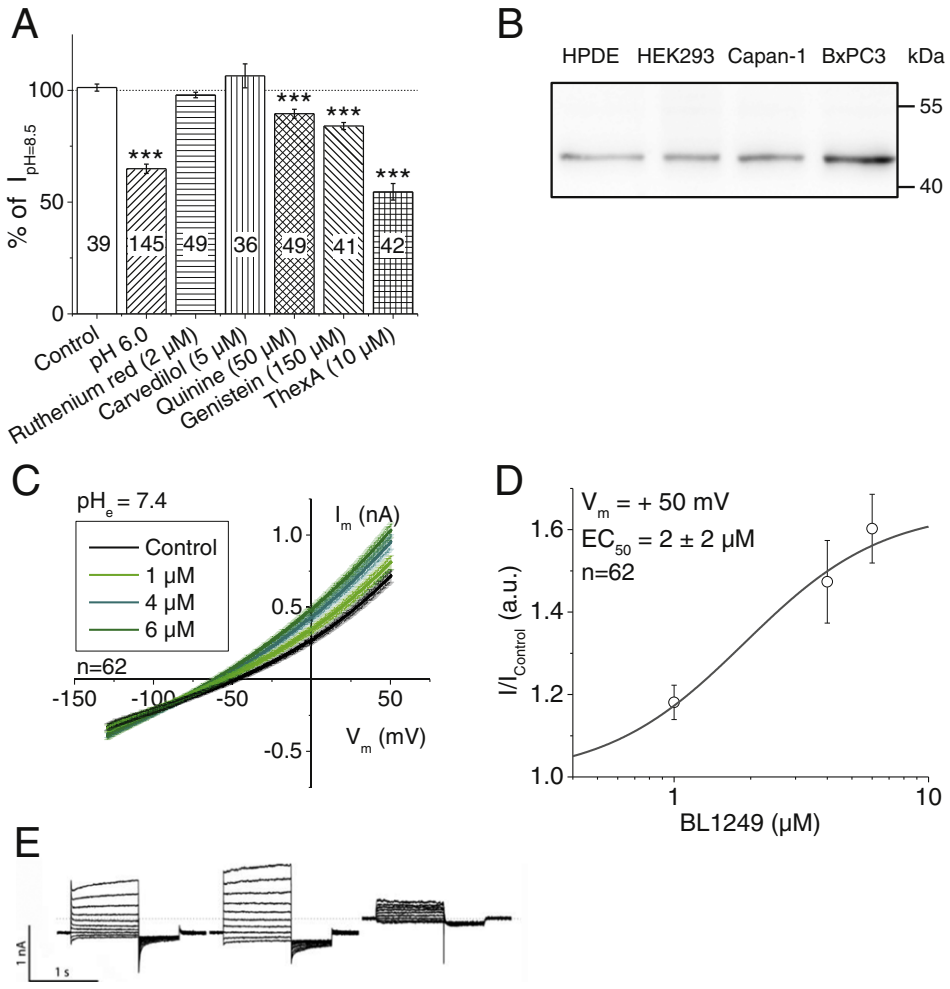

Fig. 4. pH-sensitive current in BxPC-3 cells is mediated by TREK-1. Whole-cell patch clamp recordings. A: summary of alkaline–activated (pH_e 8.5) current inhibition at $V_m = +50$ mV in presence of different K_{2P}–specific inhibitors. Control represents solution change without compound application and pH 6.0 was calculated from data of Fig. 2A as comparison. Number of cells measured is indicated on bars. B. Western blot of protein samples from the duct cell lines BxPC-3, Capan-1, and HPDE cells. HEK293 cells stably transfected with human TREK-1 served as positive control (representative of at least 3 experiments). C and D: BxPC-3 sensitivity to the activator BL1249 in physiological pH. Shown traces were recorded after full saturation of the current and data was fitted to a Hill function (D). E: representative current over time traces in presence and absence of BL1249 and the calculated BL1249–sensitive current.

(K_{ir}4.1 and K_{ir}5.1) exhibit sensitivity to different H^+ concentrations [12]. Moreover, many transient receptor potential (TRP) channels are endowed with a pH-sensing moiety [64] and a pH-induced increase in intracellular Ca^{2+} $[Ca^{2+}]_i$ could in turn activate Ca^{2+}-activated K^+ channels (K_{Ca}). However, we performed patch-clamp experiments with 0 μM Ca^{2+} and 20 mM EGTA in the pipette solution, which excludes such an indirect contribution of TRP channels and therefore K_{Ca} channels. Furthermore, 10 mM HEPES in the pipette solution kept pH_i constant and thus excludes K_{ir} channels as they only exhibit pH_i but not pH_e–dependence. K_{2P} channels do not depend solely on either of the aforementioned stimuli and further they increase open probability with substitution of intracellular K^+ by Rb^+ (Fig. 3B). K_{2P} channels are therefore the best candidates to mediate the pH–sensitive current observed in our study.

Most of the K_{2P} channels, except TREK-2 (K_{2P}10.1), are activated at alkaline and inhibited at acidic pH_e-values. However, only TASK-1, TRAAK (K_{2p}4.1), TREK-1 and partially TASK-2 show steep activation in the physiological pH range (pH 7.0–7.8) [31]. TASK-3 is structurally similar to TREK-1, but shows almost complete activation at pH_e 7.4; at this pH_e the current in BxPC-3 cells showed not even half-maximal activation. Out of the above mentioned group of candidates, only TREK-1 increases channel open probability with decreasing pH_i values in a range as we recorded in BxPC-3 cells (Fig. 3A) [47,48]. Therefore, the observed biophysical characteristics are best described by TREK-1.

The finding that TREK-1 carries the main component of pH-sensitive current is further supported by the pharmacological profile. Ruthenium red is an inhibitor of TASK-3 with $IC_{50} = 0.7$ μM [11], TREK-2 ($IC_{50} =$ 0.2 μM) and TRAAK ($IC_{50} = 1.7$ μM), and is ineffective on TREK-1 [4]. In line with this, ruthenium red showed no inhibition of pH–sensitive current when assessed at 2 μM (Fig. 4A). Traditionally, carvedilol is used as a non-selective β-adrenoceptor antagonist but was recently reported to also inhibit TASK-1 with $IC_{50} = 0.83$ μM when heterologously expressed in CHO cells [56]. Carvedilol showed no inhibition in our recordings. Quinine was shown to inhibit TRESK (K_{2P}18.1) with $IC_{50} > 100$ μM [51], TREK-1 and TWIK-1 (K_{2P}1.1) with IC_{50} values of 42 μM and 50–85 μM, respectively [32,65]. Application of 50 μM Quinine resulted in about 30% inhibition of pH_e-sensitive current. The tyrosine kinase inhibitor, genistein was reported to potentiate the ΔF508-CFTR channel activity [24] and furthermore to inhibit a multitude of channels including the viral ion channel VPU of HIV [52], L-type Ca^{2+} channel [3], TASK-1 ($IC_{50} = 12.3$ μM) and Task-3, but it was reported to be ineffective on TREK-1-mediated current at 100 μM when heterologously expressed in *Xenopus laevis* oocytes [19]. Application of 150 μM genistein attenuated pH_e-sensitive current by ≈45% in BxPC-3 cells. The unspecific nature of genistein raises the possibility of an indirect inhibition of TREK-1 and we did not further investigate this phenomenon. Tetrahexylammonium chloride (THexA) inhibits TRESK ($IC_{50} = 0.5$ μM), TREK-1 ($IC_{50} = 1$ μM) and TASK-3 ($IC_{50} = 0.2$ μM)

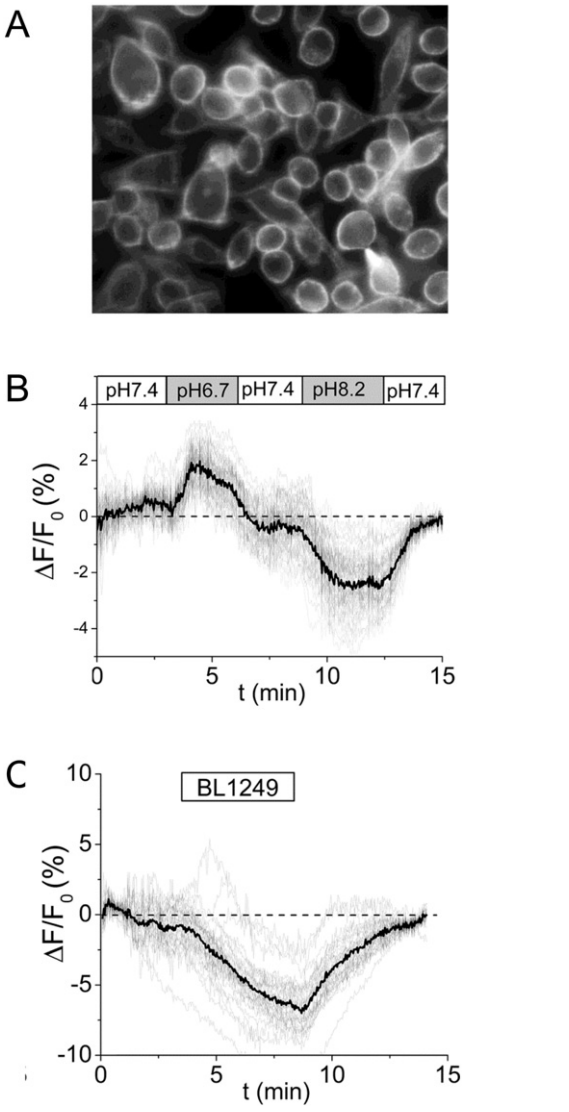

Fig. 5. pH_e and BL1249 regulate V_m. V_m was measured as change in fluorescence of the voltage-sensitive dye VF2.1.Cl. Change of $\Delta F/F_0 = 1\%$ translates to $\Delta V_m = 40–50$ mV [7,41]. Representative experiment with single cell traces shown as grey lines and average of all cells as bold black line. Each experiment was repeated in 3 independent preparations. A: representative image of VF2.1.Cl loaded BxPC-3 cells. B: cells were exposed to physiological-like solution of different pH-values as indicated. C: V_m response to application of TREK-1-specific activator BL1249 (10 μM) at pH_e 6.7.

[48], when applied intracellularly. 10 μM THexA completely inhibited pH-activated outward current (Fig. 4A) and inward current (Fig. 3C). Finally, BL1249 is an activator of endogenous TREK-1 (EC_{50} = 1.26–1.49 μM) in bladder cells [59], and it activated a K^+ current (EC_{50} of 2 ± 2 μM) in BxPC-3 cells and hyperpolarized V_m in time-lapse fluorescence experiments. All characteristics together clearly identify TREK-1 as main component of pH-regulated current in BxPC-3 cells; and the protein is expressed in PDAC cells (Fig. 4B).

4.2. BL1249 inhibits cell proliferation and migration

A relation between cancer cell proliferation and V_m was first proposed in 1971 by Cone and was since supported by many studies [9]. Highly proliferative tumor cells show generally a depolarized V_m, whereas quiescent cells are hyperpolarized [9,63]. K_{2P} channels are key players in setting V_m and are regulated by pH, a property commonly dysregulated in tumors [61]. Therefore, one can put forward a simple hypothesis that a change in pH_e from a physiological value of 7.4 to pH_e 6.7–7.1 in tumors deactivates K_{2P} channels, which in turn depolarizes V_m and thereby promotes cancer progression. We clearly demonstrated that BxPC-3 cells exhibit pH-sensitive current that plays a major role in setting V_m (Figs. 2B and 5). Following this hypothesis, one would have expected a higher proliferative rate of BxPC-3 cells at tumor-like pH values and reduced growth when exposed to activator compound BL1249. We did not find such a clear connection (Fig. 6A). Cells cultured at acidic pH 6.5 and 6.7 showed a significantly lower proliferative rate when compared to the physiological control condition (pH 7.4), though at pH 7.0, which may be expected at tumor sites, proliferation was as high as in pH 7.4 (Fig. 6A). Results obtained at pH 8.2 and pH 8.5 as well as in presence of BL1249 are in agreement with the aforementioned hypothesis – both conditions result in a hyperpolarized V_m and decreased proliferative rate (Fig. 6A and B). Interestingly, at pH_e 8.5 or in presence of BL1249 (>6 μM) TREK-1 is constitutively opened (Figs. 2A and 4D). However, BL1249 at 100 μM almost completely inhibited cell proliferation, whereas proliferation of cells cultured at pH 8.5 was only partially impaired. Since TREK-1 activation decreases proliferation, the opposite effect may be expected when the channel expression is inhibited. In our study, siRNA-induced knockdown of TREK-1 lead to a slight increase in BrdU incorporation compared to the negative control RNA (Fig. 7A) suggesting that inhibition of TREK-1 may be promotive of tumor growth (Fig. 7). However, BxPC-3 cells were affected by the treatment with siRNA, and thus we strived to use the lowest possible siRNA concentration. This may explain why we only observe a relatively moderate reduction in the protein level. TREK-1 shows complex gating with sensitivity to numerous stimuli including heat, pressure, lipids, protein kinase A (PKA) and protein kinase C (PKC), as well as cyclic adenosine monophosphate (cAMP) [22] and some of those gating mechanisms are synergistically linked [37]. This could provide an explanation for the above phenomena; pH_e-activation of TREK-1 may be dominated by other gating mechanism (see above). Furthermore, many proteins have characteristic pH optimum at physiological pH values, with decreased activity in alkaline and acid range. For example, the most important determinant of ion fluxes through ion channels is the Na^+, K^+-ATPase that has characteristic pH optimum at pH 7 [50].

Nevertheless, TREK-1 activation by BL1249 and presumably hyperpolarization of V_m is detrimental to cell proliferation, while knockdown of TREK-1 seemed to increase proliferation. In line with this suggestion is the observation that in MG63 cells pharmacological inhibition of TREK-1 channel using bupivacaine resulted in an elevated growth rate [23]. Taken together, pH-regulated V_m plays some role in BxPC-3 cell proliferation, however, a strong effect may be overlaid/attenuated by other pH-dependent regulators of proliferation [61]. Similar behavior was observed in MG63 human osteoblast-like cells, where proliferation was completely inhibited at pH 6.4 [34].

We observed pH-regulated K^+ current in 1/3 of the measured BxPC-3 cells in patch-clamp recordings. However, using the voltage-sensitive reporter dye VF2.1.Cl we found pH-dependence of V_m in all BxPC-3 cells tested. The same applies to BL1249-sensitive currents. This discrepancy may be due to differences in cell conditions in the two experimental set ups. We performed patch-clamp recordings in the whole cell configuration; this includes a complete exchange of the intracellular solution with the pipette solution. Critical components of TREK-1 channel gating or other cellular regulators may be washed out as discussed above. In V_m reporter experiments, plasma cell membranes and intracellular environment would have remained more intact.

In cell migration, K^+ channel's role in setting V_m is also important as V_m provides the electrochemical driving force for Cl^- and Ca^{2+} transport and intracellular Ca^{2+} is a key signaling ion in migration, while Cl^- channels are important in cell volume regulation. Moreover, K^+ channels are also required for volume-regulation, a pivotal function in cell migration [54]. We found no simple correlation between wound closure in scratch assays and pH-sensitive current (Figs. 2A and 6).

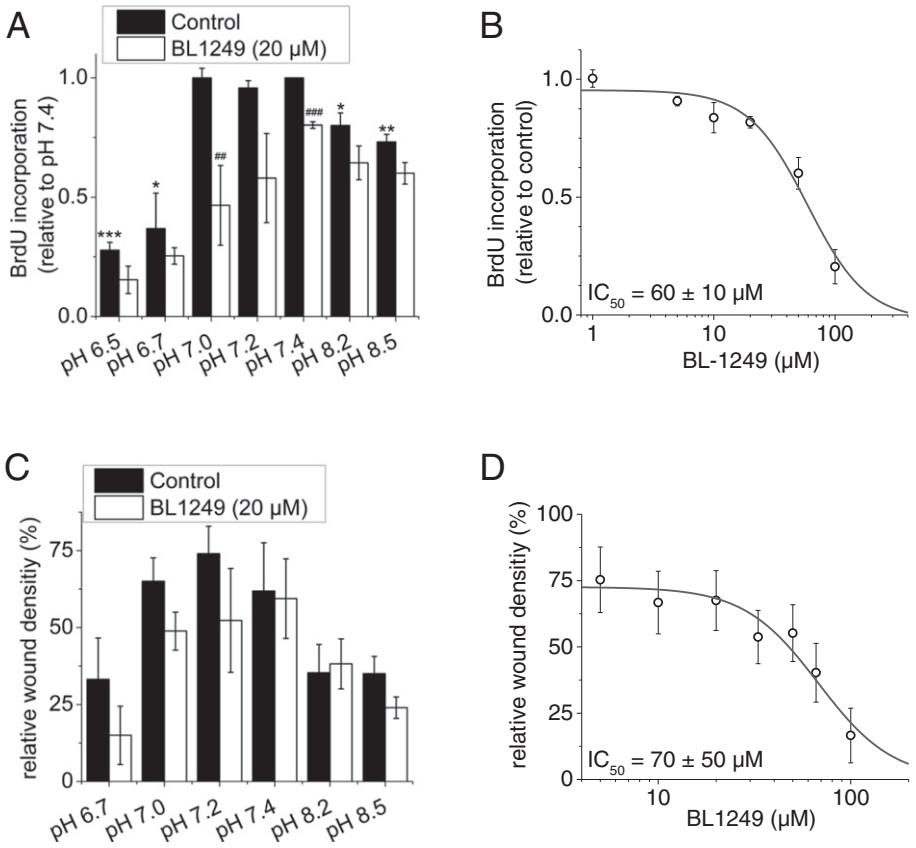

Fig. 6. BL1249 inhibits BxPC-3 cell proliferation. Cells were exposed to different pH-values and/or concentrations of BL1249 for 24 h before BrdU – incorporation was determined. Data shown represent the mean of n = 3–4 experiments ± s.e.m. A: pH-dependence of cell proliferation. * = P ≤ 0.05; ** and ## = P ≤ 0.01; *** and ### = P ≤ 0.001. * shows comparison with control condition of pH 7.4 and # indicates significance when compared with respective control condition. B: dose-response curve of BL1249 in pH 7.4. Data was fitted to a Hill function. C and D: Scratch wound healing assay of BxPC-3 cells in different pH-values and/or concentrations of BL1249 after 48 h. 5 μM aphidicolin was added to inhibit cell proliferation. Data shown represent the mean of n = 3–4 experiments ± s.e.m. C: pH-dependence of cell migration. D: dose-response curve of BL1249 at pH 7.4. Data was fitted to a Hill function.

Similar to cell proliferation, cell migration appeared to be attenuated both at acidic pH 6.7 and alkaline pH 8.2 and 8.5, however, these findings were not significant at $P < 0.05$. It is known that many processes in the migratory cascade depend on pH (e.g. formation of actin filaments [40], the GTPase CDC42 activity that is important for polarity of migrating cells [17], and of course ion transport that is regulated by pH sensitive Na^+, K^+-ATPase (see above). The effect of TREK-1 on migration may therefore be overshadowed by these processes. Nevertheless, it seems that again BL1249 attenuated cell migration at several pH_e values and there was a clear concentration-dependent inhibitory effect of BL1249 (at pH 7.4) on cell migration (Fig. 6D).

BL1249 inhibits cell proliferation as well as migration with $IC_{50} = 60 \pm 10$ and 70 ± 50 μM, respectively (Fig. 6B and D). These values are far higher than $EC_{50} = 2 \pm 2$ μM of current activation in patch clamp recordings (Fig. 4D). A possible explanation for this could be binding of the compound to the serum, which was only used in the long-term cell behavior experiments but not in electrophysiology and fluorescence microscopy experiments. To our knowledge, BL1249 has not yet been studied in serum containing media before. The similar IC_{50} of BL1249 in proliferation and migration suggests a common underlying mechanism. As described above, V_m and also volume-regulation are pivotal in both proliferation and migration; a constitutively activated TREK-1 channel may impair either or both of these processes.

Many studies found expression of different K_{2P} channels including TALK-1 and 2 [15], TASK-1 and 2 [16] TASK-5 [2], TRESK-2 [26] TREK-2 [33] TWIK-2 [49] in the pancreas using analysis of mRNA. So far, only one study investigated K_{2P} expression in pathological state of the pancreas. Using a data-mining approach, Williams et al. found in this study a significant downregulation of TASK-1 and upregulation of TWIK-1 mRNA in tissues of PDAC patients when compared with unaffected tissue of same origin [62]. For the first time, we identified TREK-1 as major component in the PDAC cell line BxPC-3. However, no pH-regulated K^+ current was detected in the PDAC cell lines Capan-1, AsPC-1 as well as HPDE cells in patch clamp experiments; these cells have very little K^+ conductance (Supplementary Fig. S1). Yet these cells express TREK-1 channels, which may be closed but activate-able by BL1249, as shown by the fluorescence measurements with VF2.1.Cl on Capan-1 and HPDE cells. These experiments also revealed that these cells exhibited different relation between extracellular pH and V_m (Supplementary Fig. S2). This behavior matches the biology of TREK-2, but other, for example pH sensitive Cl^- channels, cannot be excluded. Capan-1 and AsPC-1 are derived from liver metastasis and ascites, respectively. On the other hand, BxPC-3 cells originate from adenocarcinoma of the body of the pancreas where the patient presented no signs of metastasis [13]. Therefore, TREK-1 expression might be related to different development stages of the cancer. Furthermore, in other PDAC cells there is an indication that V_m is dominated by Cl^- conductance (Fig. S1) and TMEM16A is expressed in these cells [53].

In conclusion, we found a pH-sensitive K^+ current in BxPC-3 cells that exhibits biophysical and pharmacological characteristics as described for TREK-1. We further showed that this current plays a crucial role in setting V_m. Moreover, we identified BL1249, activator of TREK-1, as potential inhibitor of both pancreatic cancer cell proliferation and migration; it may therefore be an interesting compound for further optimization.

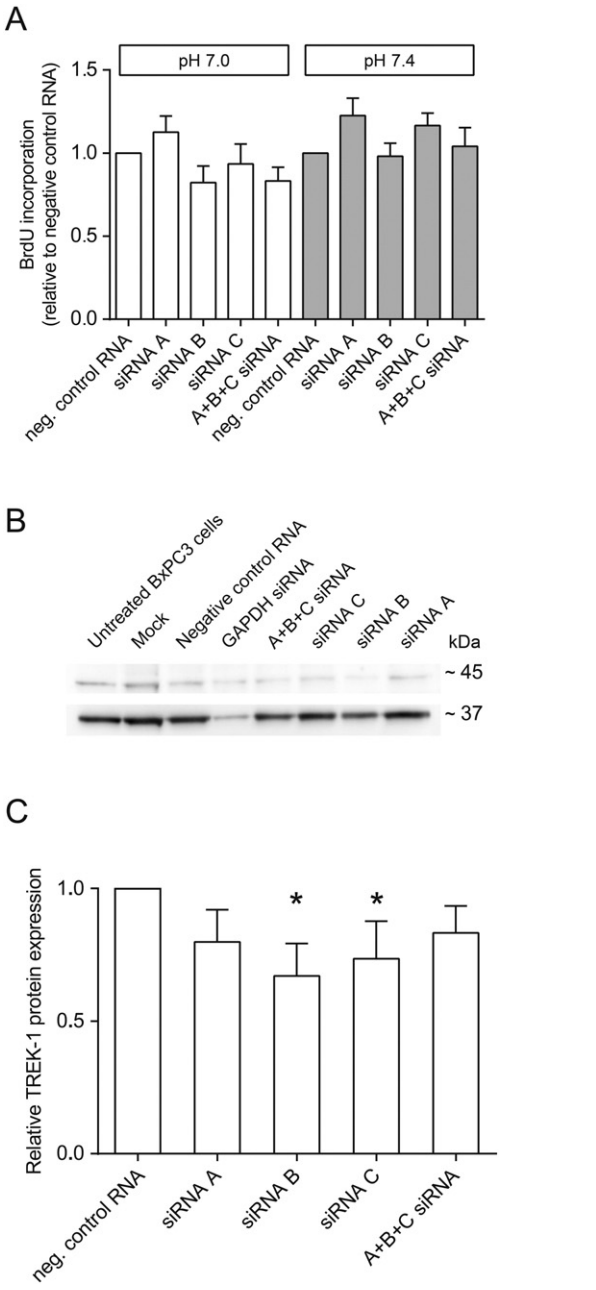

Fig. 7. Effect of siRNA mediated knockdown of TREK-1 on cell proliferation. Cells were transfected with siRNA at a final concentration of 25 nM three days prior to determination of BrdU incorporation. A: at pH 7.4 there was a tendency towards increased BrdU incorporation relative to negative (neg.) control RNA ($P = 0.065$ for siRNA A and $P = 0.059$ for siRNA C). Data show the mean ± s.e.m. from $n = 5$ experiments. B: knockdown of TREK-1 by the different siRNAs was also assayed by Western Blot analysis 3 to 4 days after transfection. For TREK-1 protein level analysis, the band at 45 kDa was used (upper lane) and for GAPDH protein the band at 37 kDa was analyzed (lower lane). GAPDH siRNA served as positive control for transfection. C: densitometric analysis of TREK-1 expression normalized to GAPDH after transfection with the different siRNAs. Data show the mean ± s.e.m. from 5 independent transfections.* indicates $P \leq 0.05$ relative to samples from negative control RNA transfected cells.

Supplementary data to this article can be found online at http://dx.doi.org/10.1016/j.bbadis.2016.07.009.

Conflicts of interest

Andrea Brüggemann and Markus Rapedius are employees of Nanion Technology GmbH.

Ethical standards

All experiments were carried out in compliance to the current laws of the country.

Transparency document

The Transparency document associated with this article can be found, in online version.

Acknowledgements

This work was supported by the Marie Curie Initial Training Network *IonTraC* (Grant Agreement No. 289648). Further support was from the Novo Nordisk Foundation (NFF13OC0007353), the Lundbeck Foundation (R173-2014-1462) and The Danish Council for Independent Research | Natural Sciences (DFF 4002-00162). We thank Dr. R.Y. Tsien, a Howard Hughes Medical Institute Investigator at the University of California San Diego, for the generous gift of VF2.1.Cl. H6c7 cell line was a kind gift of Dr. M-S. Tsao from University Health Network in Toronto. HEK293 cells expressing human TREK-1 were a kind gift of Dr. Charlotte Hougaard from Neurosearch. The authors thank Pernille Roshof and Helle Walas for technical assistance.

References

[1] C.P. Alvarez-Baron, P. Jonsson, C. Thomas, S.E. Dryer, C. Williams, The two-pore domain potassium channel KCNK5: induction by estrogen receptor alpha and role in proliferation of breast cancer cells, Mol. Endocrinol. 25 (2011) 1326–1336.
[2] I. Ashmole, P. Goodwin, P.R. Stanfield, TASK-5, a novel member of the tandem pore K^+ channel family, Pflugers Arch. - Eur. J. Physiol. 442 (2001) 828–833.
[3] A.E. Belevych, S. Warrier, R.D. Harvey, Genistein inhibits cardiac L-type Ca^{2+} channel activity by a tyrosine kinase-independent mechanism, Mol. Pharmacol. 62 (2002) 554–565.
[4] G. Braun, M. Lengyel, P. Enyedi, G. Czirják, Differential sensitivity of TREK-1, TREK-2 and TRAAK background potassium channels to the polycationic dye ruthenium red, Br. J. Pharmacol. 172 (2015) 1728–1738.
[5] E. Bulk, A. Ay, M. Hammadi, H. Ouadid-ahidouch, A. Hascher, C. Rohde, N.H. Thoennissen, E. Schmidt, A. Marra, L. Hillejan, A.H. Jacobs, H. Klein, M. Dugas, W.E. Berdel, C. Müller-tidow, A. Schwab, Epigenetic dysregulation of KCa3.1 channels induces poor prognosis in lung cancer, Int. J. Cancer (2015), http://dx.doi.org/10.1002/ijc.29490.
[6] S. Cascinu, M. Falconi, V. Valentini, S. Jelic, Pancreatic cancer: ESMO clinical practice guidelines for diagnosis, treatment and follow-up, Ann. Oncol. 21 (2010) 55–58.
[7] F. Ceriani, F. Mammano, A rapid and sensitive assay of intercellular coupling by voltage imaging of gap junction networks, Cell Commun. Signal. 11 (2013) 78.
[8] K. Choi, C. Mossman, A. Jeffrey, G. Yellen, The internal quaternary ammonium of shaker potassium channels, Cell 10 (1993) 533–541.
[9] C.D. Cone, Unified theory on the basic mechanism of normal mitotic control and oncogenesis, J. Theor. Biol. 30 (1971) 151–181.
[10] V.A. Cuddapah, H. Sontheimer, Ion channels and transporters in cancer. 2. Ion channels and the control of cancer cell migration, Am. J. Physiol. Cell Physiol. 301 (2011) C541–C549.
[11] G. Czirják, P. Enyedi, Ruthenium red inhibits TASK-3 potassium channel by interconnecting glutamate 70 of the two subunits, Mol. Pharmacol. 63 (2003) 646–652.
[12] M.C. D'Adamo, L. Shang, P. Imbrici, S.D.M. Brown, M. Pessia, S.J. Tucker, Genetic inactivation of Kcnj16 identifies Kir5.1 as an important determinant of neuronal PCO_2/pH sensitivity, J. Biol. Chem. 286 (2011) 192–198.
[13] E.L. Deer, J. González-Hernández, J.D. Coursen, J.E. Shea, J. Ngatia, C.L. Scaife, M.A. Firpo, S.J. Mulvihill, Phenotype and genotype of pancreatic cancer cell lines, Pancreas 39 (2010) 425–435.
[14] J. Dunlop, M. Bowlby, R. Peri, D. Vasilyev, R. Arias, High-throughput electrophysiology: an emerging paradigm for ion-channel screening and physiology, Nat. Rev. Drug Discov. 7 (2008) 358–368.
[15] F. Duprat, C. Girard, G. Jarretou, M. Lazdunski, Pancreatic two P domain K^+ channels TALK-1 and TALK-2 are activated by nitric oxide and reactive oxygen species, J. Physiol. 562 (2005) 235–244.
[16] F. Duprat, F. Lesage, M. Fink, R. Reyes, C. Heurteaux, M. Lazdunski, TASK, a human background K^+ channel to sense external pH variations near physiological pH, EMBO J. 16 (1997) 5464–5471.
[17] C. Frantz, A. Karydis, P. Nalbant, K.M. Hahn, D.L. Barber, Positive feedback between Cdc42 activity and H^+ efflux by the Na-H exchanger NHE1 for polarity of migrating cells, J. Cell Biol. 179 (2007) 403–410.
[18] T. Furukawa, W. Duguid, L. Rosenberg, J. Viallet, D. Galloway, M. Tsao, Short communication long-term culture and immortalization of epithelial cells from normal adult human, Am. J. Pathol. 148 (1996) 1763–1770.

[19] J. Gierten, E. Ficker, R. Bloehs, K. Schlömer, S. Kathöfer, E. Scholz, E. Zitron, C. Kiesecker, A. Bauer, R. Becker, H. Katus, C. Karle, D. Thomas, Regulation of two-pore-domain (K2P) potassium leak channels by the tyrosine kinase inhibitor genistein, Br. J. Pharmacol. 154 (2008) 1680–1690.

[20] R.J. Gillies, N. Raghunand, G.S. Karczmar, Z.M. Bhujwalla, MRI of the tumor microenvironment, J. Magn. Reson. Imaging 16 (2002) 430–450.

[21] M. Hayashi, I. Novak, Molecular basis of potassium channels in pancreatic duct epithelial cells, Channels 7 (2013) 432–441.

[22] E. Honoré, The neuronal background K2P channels: focus on TREK1, Nat. Rev. Neurosci. 8 (2007) 251–261.

[23] S. Hughes, J. Magnay, M. Foreman, S.J. Publicover, J.P. Dobson, A.J. El Haj, Expression of the mechanosensitive 2PK$^+$ channel TREK-1 in human osteoblasts, J. Cell. Physiol. 206 (2006) 738–748.

[24] T.C. Hwang, F. Wang, I.C. Yang, W.W. Reenstra, Genistein potentiates wild-type and DeltaF508-CFTR channel activity, Am. J. Physiol. Cell Physiol. 273 (1997) C988–C998.

[25] H. Jäger, T. Dreker, A. Buck, K. Giehl, T. Gress, S. Grissmer, Blockage of intermediate-conductance Ca^{2+}-activated K^+ channels inhibit human pancreatic cancer cell growth in vitro, Mol. Pharmacol. 65 (2004) 630–638.

[26] D. Kang, E. Mariash, D. Kim, Functional expression of TRESK-2, a new member of the tandem-pore K^+ channel family, J. Biol. Chem. 279 (2004) 28063–28070.

[27] C.J. Kim, Y.G. Cho, S.W. Jeong, Y.S. Kim, S.Y. Kim, S.W. Nam, S.H. Lee, N.J. Yoo, J.Y. Lee, W.S. Park, Altered expression of KCNK9 in colorectal cancers, APMIS 112 (2004) 588–594.

[28] I. Lauritzen, M. Zanzouri, E. Honoré, F. Duprat, M.U. Ehrengruber, M. Lazdunski, A.J. Patel, K^+-dependent cerebellar granule neuron apoptosis. Role of TASK leak K^+ channels, J. Biol. Chem. 278 (2003) 32068–32076.

[29] G.-W. Lee, H.S. Park, E.-J. Kim, Y.-W. Cho, G.-T. Kim, Y.-J. Mun, E.-J. Choi, J.-S. Lee, J. Han, D. Kang, Reduction of breast cancer cell migration via up-regulation of TASK-3 two-pore domain K^+ channel, Acta Physiol (Oxford) 204 (2012) 513–524.

[30] J.M. Lee, F.M. Davis, S.J. Roberts-Thomson, G.R. Monteith, Ion channels and transporters in cancer. 4. Remodeling of Ca^{2+} signaling in tumorigenesis: role of Ca^{2+} transport, Am. J. Physiol. Cell Physiol. 301 (2011) C969–C976.

[31] F. Lesage, J. Barhanin, Molecular physiology of pH-sensitive background K(2P) channels, Physiology 26 (2011) 424–437.

[32] F. Lesage, E. Guillemare, M. Fink, F. Duprat, M. Lazdunski, G. Romey, J. Barhanin, TWIK-1, a ubiquitous human weakly inward rectifying K^+ channel with a novel structure, EMBO J. 15 (1996) 1004–1011.

[33] F. Lesage, C. Terrenoire, G. Romey, M. Lazdunski, Human TREK2, a 2P domain mechano-sensitive K^+ channel with multiple regulations by polyunsaturated fatty acids, lysophospholipids, and Gs, Gi, and Gq protein-coupled receptors, J. Biol. Chem. 275 (2000) 28398–28405.

[34] X. Li, X. Dong, S. Zheng, J. Xiao, Expression and localization of TASK-1, -2 and -3 channels in MG63 human osteoblast-like cells, Oncol. Lett. 5 (2012) 865–869.

[35] A. Litan, S. Langhans, Cancer as a channelopathy: ion channels and pumps in tumor development and progression, Front. Cell. Neurosci. 9 (2015) 1–11.

[36] D.P. Lotshaw, Biophysical, pharmacological, and functional characteristics of cloned and native mammalian two-pore domain K^+ channels, Cell Biochem. Biophys. 47 (2007) 209–256.

[37] F. Maingret, J. Patel, F. Lesage, M. Lazdunski, E. Honore, Mechano- or acid stimulation, two interactive modes of activation of the TREK-1 potassium channel, J. Biol. Chem. 274 (1999) 26691–26696.

[38] C. Martin, S. Pedersen, Intracellular pH gradients in migrating cells, Am. J. Physiol. Cell Physiol. 300 (2011) 490–495.

[39] A. Masi, A. Becchetti, R. Restano-Cassulini, S. Polvani, G. Hofmann, M. Buccoliero, M. Paglierani, B. Pollo, G.L. Taddei, P. Gallina, N. Di Lorenzo, S. Franceschetti, E. Wanke, A. Arcangeli, hERG1 channels are overexpressed in glioblastoma multiforme and modulate VEGF secretion in glioblastoma cell lines, Br. J. Cancer 93 (2005) 781–792.

[40] G.D. McLachlan, S.M. Cahill, M.E. Girvin, S.C. Almo, Acid-induced equilibrium folding intermediate of human platelet profilin, Biochemistry 46 (2007) 6931–6943.

[41] Miller EW, Lin JY, Frady EP, Steinbach PA, Kristan WB, Tsien RY. Optically monitoring voltage in neurons by photo- induced electron transfer through molecular wires. Proc. Natl. Acad. Sci.

[42] D. Mu, L. Chen, X. Zhang, L. See, C.M. Koch, C. Yen, J.J. Tong, L. Spiegel, K.C.Q. Nguyen, A. Servoss, Y. Peng, L. Pei, J.R. Marks, S. Lowe, T. Hoey, L.Y. Jan, W.R. Mccombie, M.H. Wigler, S. Powers, Genomic amplification and oncogenic properties of the KCNK9 potassium channel gene, Cancer Cell 3 (2003) 297–302.

[43] D. Nagy, M. Gönczi, B. Dienes, Á. Szöőr, J. Fodor, Z. Nagy, A. Tóth, T. Fodor, P. Bai, G. Szücs, Z. Rusznák, L. Csernoch, Silencing the KCNK9 potassium channel (TASK-3) gene disturbs mitochondrial function, causes mitochondrial depolarization, and induces apoptosis of human melanoma cells, Arch. Dermatol. Res. 306 (2014) 885–902.

[44] D. Oliver, H. Hahn, C. Antz, J.P. Ruppersberg, B. Fakler, Interaction of permeant and blocking ions in cloned inward-rectifier K^+ channels, Biophys. J. 74 (1998) 2318–2326.

[45] H. Ouyang, L. Mou, C. Luk, N. Liu, J. Karaskova, J. Squire, M.S. Tsao, Immortal human pancreatic duct epithelial cell lines with near normal genotype and phenotype, Am. J. Pathol. 157 (2000) 1623–1631.

[46] L. Pardo, W. Stühmer, The roles of K^+ channels in cancer, Nat. Rev. Cancer 14 (2014) 39–48.

[47] A. Patel, E. Honoré, Properties and modulation of mammalian 2P domain K^+ channels, Trends Neurosci. 24 (2001) 339–346.

[48] P.L. Piechotta, M. Rapedius, P.J. Stansfeld, M.K. Bollepalli, G. Ehrlich, G. Erhlich, I. Andres-Enguix, H. Fritzenschaft, N. Decher, M.S.P. Sansom, S.J. Tucker, T. Baukrowitz, The pore structure and gating mechanism of K2P channels, EMBO J. 30 (2011) 3607–3619.

[49] D.J. Pountney, I. Gulkarov, E. Vega-Saenz De Miera, D. Holmes, M. Saganich, B. Rudy, M. Artman, Coetzee W A, Identification and cloning of TWIK-originated similarity sequence (TOSS): a novel human 2-pore K^+ channel principal subunit, FEBS Lett. 450 (1999) 191–196.

[50] F. Romero, Solubilization and partial characterization of ouabain-insensitive Na(+)-ATPase from basolateral plasma membranes of the intestinal epithelial cells, Investig. Clin. 50 (2009) 303–314.

[51] Y. Sano, K. Inamura, A. Miyake, S. Mochizuki, C. Kitada, H. Yokoi, K. Nozawa, H. Okada, H. Matsushime, K. Furuichi, A novel two-pore domain K^+ channel, TRESK, is localized in the spinal cord, J. Biol. Chem. 278 (2003) 27406–27412.

[52] D. Sauter, S. Schwarz, K. Wang, R. Zhang, B. Sun, W. Schwarz, Genistein as antiviral drug against HIV ion channel, Planta Med. 80 (2014) 682–687.

[53] D.R.P. Sauter, I. Novak, S.F. Pedersen, E.H. Larsen, E.K. Hoffmann, ANO1 (TMEM16A) in pancreatic ductal adenocarcinoma (PDAC), Pflugers Arch. 467 (2015) 1495–1508.

[54] A. Schwab, A. Fabian, P.J. Hanley, C. Stock, Role of ion channels and transporters in cell migration, Physiol. Rev. 92 (2012) 1865–1913.

[55] F.V. Sepulveda, L. Pablo Cid, J. Teulon, M.I. Niemeyer, Molecular aspects of structure, gating, and physiology of pH-sensitive background K2P and Kir K^+-transport channels, Physiol. Rev. 95 (2014) 179–217.

[56] K. Staudacher, I. Staudacher, E. Ficker, C. Seyler, J. Gierten, J. Kisselbach, A.-K. Rahm, K. Trappe, P. Schweizer, R. Becker, H. Katus, D. Thomas, Carvedilol targets human K2P 3.1 (TASK1) K^+ leak channels, Br. J. Pharmacol. 163 (2011) 1099–1110.

[57] L. Stüwe, M. Müller, A. Fabian, J. Waning, S. Mally, J. Noël, A. Schwab, C. Stock, pH dependence of melanoma cell migration: protons extruded by NHE1 dominate protons of the bulk solution, J. Physiol. 585 (2007) 351–360.

[58] D. Sun, R. Urrabaz, C. Buzello, M. Nguyen, Induction of DNA ligase I by 1-β-D-arabinosylcytosine and aphidicolin in MiaPaCa human pancreatic cancer cells, Exp. Cell Res. 280 (2002) 90–96.

[59] S. Tertyshnikova, R.J. Knox, M.J. Plym, G. Thalody, C. Griffin, T. Neelands, D.G. Harden, L. Signor, D. Weaver, R.A. Myers, N.J. Lodge, T NDDS, Discovery L, Profiling RJK, BL-1249 [(5,6,7,8-tetrahydro-naphthalen-1-yl)-[2-(1H-tetrazol-5-yl)-phenyl]-amine]: a putative potassium channel opener with bladder-relaxant properties, J. Pharmacol. Exp. Ther. 313 (2005) 250–259.

[60] I. Voloshyna, A. Besana, M. Castillo, T. Matos, I.B. Weinstein, M. Mansukhani, R.B. Robinson, C. Cordon-Cardo, S.J. Feinmark, TREK-1 is a novel molecular target in prostate cancer, Cancer Res. 68 (2008) 1197–1203.

[61] B. Webb, M. Chimenti, M.P. Jacobson, D.L. Barber, Dysregulated pH: a perfect storm for cancer progression, Nat. Rev. Cancer 11 (2011) 671–677.

[62] S. Williams, A. Bateman, I. O'Kelly, Altered expression of two-pore domain potassium (K2P) channels in cancer, PLoS One 8 (2013), e74589.

[63] M. Yang, W.J. Brackenbury, Membrane potential and cancer progression, Front. Physiol. 4 (2013) 1–10.

[64] J. Zheng, Molecular mechanism of TRP channels, Compr. Physiol. 3 (2013) 221–242.

[65] M. Zhou, G. Xu, M. Xie, X. Zhang, G.P. Schools, L. Ma, H.K. Kimelberg, H. Chen, TWIK-1 and TREK-1 are potassium channels contributing significantly to astrocyte passive conductance in rat hippocampal slices, J. Neurosci. 29 (2009) 8551–8564.